Pneumatic angle adjustment for magic angle spinning spherical rotors

Journal of Magnetic Resonance Open 6–7 (2021) 100014

Contents lists available at ScienceDirect

Journal of Magnetic Resonance Open

journal homepage: www.elsevier.com/locate/jmro

Research Article

Pneumatic angle adjustment for magic angle spinning spherical rotors

Thomas M. Osborn Popp*, Nicholas H. Alaniva, Ronny Gunzenhauser, Pin-Hui Chen, Chukun Gao, Lauren E. Price, Alexander B. Barnes

Laboratory for Physical Chemistry, ETH Zürich, Vladimir-Prelog-Weg 2, 8093 Zürich, Switzerland

ARTICLE INFO

Keywords:
Angle adjustment
Spherical rotors
MAS
Pneumatic
NMR hardware
Solid state NMR

ABSTRACT

Precise alignment of the sample's spinning axis is vital for many magic angle spinning solid state NMR experiments. Spherical rotors are a new paradigm for magic angle spinning NMR, having been demonstrated to spin stably with little risk of rotor crash, but like cylindrical rotors, they have previously only utilized a mechanical adjustment method to set the sample's rotation axis to the magic angle. Here we show that by using a second gas aperture within the stator, a spherical rotor's axis of rotation may be precisely pitched about the magic angle without mechanical adjustment or motion of the stator. The ^{2}H MAS sideband lineshape of the carboxylic acid deuteron resonance in d_4-malonic acid is used as a measure of the rotor's absolute deviation above or below the magic angle by comparing the experimental data to simulated lineshapes. We observe a linear, monotonic relationship between the angle adjustment gas flow rate and the rotor's pitch angle, which is also accompanied by an increase in spinning rate. Precise and *in operando* control of the spinning axis angle is expected to have considerable advantages to future implementation of MAS within narrow-bore magnets, and for variable angle spinning (VAS) and dynamic angle spinning (DAS) experiments.

Introduction

A necessary part of every solid state NMR experiment employing the technique of magic-angle spinning (MAS) is the adjustment of the rotor's spinning axis to be aligned with the magic angle, which is 54.7356^{0} with respect to the external magnetic field [1–3]. Rapidly spinning a solid sample about the magic angle yields a significant increase in resolution by averaging anisotropic spin interactions such as the chemical shift anisotropy, dipolar coupling, and quadrupolar coupling to first order [4–7]. To date, solid state MAS NMR probes have generally employed a mechanical angle adjustment method for setting the sample to the magic angle, where the linear motion of a threaded rod pitches the stator about an axis perpendicular to the magnetic field. While simple and effective, the mechanical adjustment system can be quite problematic in cryogenic MAS due to thermal contraction, and generally can take up significant volume within the probehead. This extra space is becoming increasingly valuable as more and more solid state NMR probes are being designed to fit within narrow-bore magnets. Moreover, sufficient space within probeheads is also required for RF circuitry elements, microwave components, and cryogenics for dynamic nuclear polarization (DNP) experiments [8–11]. Additionally, the requirement that the stator and coil must be able to rotate together necessitates that flexible copper leads must be used to link the RF circuit to the coil, which imposes a constraint in the RF engineering of probeheads and becomes a significant drawback at high NMR frequencies (>800 MHz) where ideally, lead lengths should be rigid and short [8,12,13]. A non-mechanical angle adjust method has been previously developed that uses a perpendicular magnetic field coil to adjust the external magnetic field vector with respect to the sample, but this method also faces challenges to implementation in cases where probehead volume is limited, and may scale inefficiently at high magnetic field strengths [14].

Spherical rotors are a promising new platform for MAS experiments, exhibiting exceptional rotational stability and resilience against crashing due to their axis of symmetry being aligned with their highest-inertia axis [15–17]. The spherical rotor rotates within a hemispherical cup, driven by gas flowing across the rotor's equator from a single aperture positioned within the cup to incline the rotor's axis of rotation to the magic angle. As there is no bearing or axle to direct the spinning angle, the rotor's rotational axis can pitch freely within the cup, and in all previous sphere MAS stator designs, the spinning axis has been adjusted mechanically by pitching the stator to move the aperture, whereby the rotor follows to maintain its symmetry axis perpendicular to the direction of the gas flow.

In order to obtain the highest quality spectra at any MAS rate, the angle at which the sample spins must be tightly controlled and adjusted to account for any orientational changes to the experimental apparatus. While most solid state NMR experiments are insensitive to magic angle offset to within a few hundredths of a degree, there are experiments which require extremely precise setting of the magic angle, such as satellite-transition MAS (ST-MAS) [18–21]. It can also be useful to in-

* Corresponding author.

https://doi.org/10.1016/j.jmro.2021.100014
Received 10 February 2021; Received in revised form 1 May 2021; Accepted 5 May 2021

tentionally spin samples at a precise angle slightly offset from the magic angle to re-introduce residual couplings [22–26]. To set the sample's rotational axis to the magic angle for a cylindrical rotor, methods have been developed to measure the angle of the stator with respect to the magnetic field, such as laser alignment and Hall effect voltage measurement [27–29]. However, the most common way to set the magic angle is by maximizing the intensity of satellite transition rotor echoes in the ^{79}Br time domain NMR signal of KBr, which is usually accurate to within about 0.1^0 of the magic angle [30]. For very precise and absolute angular measurement, the off-magic angle ^{2}H NMR lineshape of some deuterated organic solids manifests as a peak splitting which is very sensitive to magic angle offset [14,31,32]. J. Griffin et al. have demonstrated that the ^{2}H NMR signal of d_4-malonic acid is highly dependent on magic angle offset, where the residual quadrupolar interaction for the carboxylic acid deuteron (COOD) manifests off-magic angle as an asymmetric peak splitting, and the direction of the asymmetry is dependent on whether the rotor is pitched above or below the magic angle [33].

Here we demonstrate a novel pneumatic method for setting the magic angle for spherical rotors by using a second gas aperture to pitch the rotor's axis of rotation within the stator cup. Whereas previously deployed pneumatic driven spinning angle adjustment mechanisms required an intermediary mechanical movement of the stator [34], here the rotor itself is the only moving component of the apparatus. We show that the angle can be precisely controlled by adjusting the flow rate of gas through the angle adjustment aperture by measuring ^{2}H NMR spectra of d_4-malonic acid as the gas flow rate is varied. These spectra are compared to simulations in order to determine the angular precision of the method.

Experimental details

The stator for spinning spherical rotors with pneumatic angle adjustment was 3D-printed in a clear acrylonitrile-butadiene-styrene (ABS)-like polymer using a Projet MJP2500 3D printer (3D Systems, Rock Hill, SC, US). We note that this printer is relatively (10x) more expensive than commonly deployed printers such as the Form3 printer from Formlabs, but provides superb resolution. We have observed extremely good reproducibility from the Projet printer, greatly simplifying the iterative process required to optimize the stator for spinning and angle adjustment. After the stator geometry was optimized using the Projet, we have since also fabricated, using the more accessible Form3 printer, multiple stators for pneumatic angle adjustment of 9.5 mm rotors. The stator was installed into a modified double-resonance APEX-style Chemagnetics probe using a double-saddle coil for NMR signal excitation and detection as described previously [17]. A 9.5 mm rotor machined from yttria-stabilized zirconia with a 161 μL sample space and 12 0.35 mm depth 60-degree V-shaped grooves (O'Keefe Ceramics, Woodland Park, CO, US) was used for NMR experiments [15]. The rotor was packed with 180.1 mg of d_4-malonic acid (98% atom percent deuterium, Sigma Aldrich) using specially-designed rotor packing tools to ensure even distribution of material (Supplementary Information, Fig. S1), and sealed at both ends using spherically-contoured (4.75 mm radius) 3D-printed ABS-like plastic caps.

The design of the stator for pneumatic angle adjustment of the rotor's spinning axis is shown in Fig. 1. The rotor is placed into the stator cup, where the primary contribution to the angular momentum of the rotor comes from the gas flow out of the main drive aperture marked in blue. The drive aperture is centered just beyond the complement of the magic angle (145.74^0 from the vertical axis) to apply torque at the equator of the rotor, causing the rotor to spin about an axis inclined at 55.74^0 with respect to the vertical axis. The geometry of the drive aperture in this design differs from the aperture previously employed in stators for spinning spheres. This aperture geometry is designed to minimize gas flow normal to the surface of the stator cup and to maximize gas flow in the gap between the stator cup and the sphere surface, resulting in improved stability of the rotor during the spin-up and spin-down procedures. The angle adjust aperture is placed at a 90^0 angle from the vertical axis on the opposite side of the stator cup, producing gas flow in the opposite direction of the main drive gas flow. The wall of the stator cup near the angle adjust aperture was removed to allow for unimpeded expansion of the gas flow from the angle adjust aperture, with no adverse effects on the spinning stability of the rotor.

NMR experiments were performed at 7.05 T using a Bruker Avance III spectrometer (Bruker Corp., Billerica, MA, US). ^{2}H MAS spectra were taken at a transmitter frequency of 46.08 MHz using a $\pi/2$ pulse of 9 μs at 300 W incident RF power and with an inter-scan delay of 0.8 s. The ^{2}H MAS spectrum depicted in Fig. 2C was collected at an MAS rate of 6536 Hz using helium gas and processed by summing the spectra obtained by stepping the frequency across the width of the resonance. MAS was performed with either air or helium gas, where the main drive pressure was kept constant at 2 bar, and the angle adjust gas flow rate was coarsely adjusted by changing the pressure between 0 and 0.5 bar, and finely adjusted using a needle valve to further restrict the gas flow going to the stator. The angle adjust gas flow rate was monitored using a Red-y compact digital mass flow meter (Vögtlin Instruments, Switzerland). For troubleshooting purposes, the lever arm for mechanical adjustment of the rotor's pitch angle was included in the stator design, but in principle, the probehead can be configured with no mechanically adjustable parts whatsoever.

Spectra of the COOD deuteron resonance in d_4-malonic acid as a function of MAS angle offset were simulated with the SIMPSON package by calculating the evolution of the quadrupolar interaction to second order for a single spin-1 nucleus while rotating at the magic angle or slightly off the magic angle [33,35]. All simulations were performed using the 'rep678′ angle set, and with 32 gamma angles. Spectra were simulated across a range of rotor spinning axis angles at a rotation rate of 3000 Hz. Additional simulations were performed at different spinning rates (3 kHz, 30 kHz, 100 kHz) and magnetic field strengths (7 T, 21 T) (Supplementary Information, Figs. S2–S5). The simulated spectrum in Fig. 2C was simulated in DMFit using the same quadrupolar parameters (C_q and η_q) that were used for the SIMPSON calculations [36].

Results and discussion

A point force applied tangent to the surface of a sphere will induce a torque that causes the sphere to gain angular momentum about the axis associated with that torque. A second point force applied to the surface of the sphere at a different point will cause the angular momentum vector to change direction and magnitude based on the sum of the two torques on the sphere. Fig. 1C depicts two point forces applied in opposite directions tangent to a sphere along the x-axis at points that lie in the yz-plane, approximating the forces experienced by the spherical rotor in the pneumatic angle adjust stator. The resultant torque (black arrow) is aligned with the rotor's angular momentum vector, and is the orientation of the rotor's spinning axis. When only the drive force (blue arrow) is applied, the angular momentum vector is at an angle of 55.74^0 with respect to the z-axis. As the angle adjust force is increased (red arrow), the angle between the z-axis and the angular momentum vector decreases, while at the same time, the magnitude of the angular momentum vector must increase. This implies a monotonic relationship between the angle adjust gas flow rate, the spinning rate, and the angle of the rotor's rotational axis. While the forces caused by the gas flow from each aperture in the stator are not exactly perfect point forces and the motion of the rotor is complicated by other fluid dynamical phenomena, this simple model is sufficient to explain the mechanism of pneumatic angle adjustment for this configuration of the stator.

The placement of the angle adjust aperture within the stator cup is significant. In our early stator designs, we attempted to induce a pitch of the rotor's spinning axis by independently tuning the gas flow between two closely spaced drive gas apertures equally offset on either side of the magic angle complement within the stator cup. While some control over the spinning axis was possible in this design, the spinning was com-

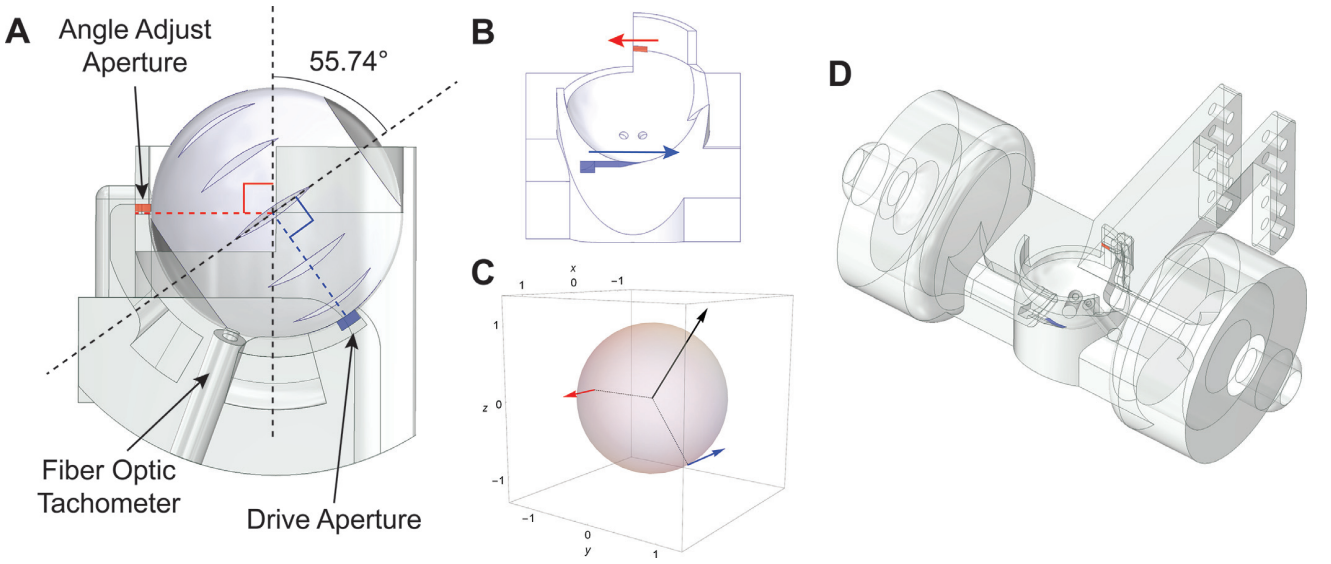

Fig. 1. Design of the pneumatic angle adjust stator for 9.5 mm spherical rotors. A) Side view of the stator cup with spherical rotor included, with the main drive aperture highlighted in blue and the angle adjust aperture highlighted in red. B) Cross-sectional view of the stator cup through the angled plane bisecting the main drive aperture, showing the directions of gas flow for the drive (blue arrow) and the angle adjust (red arrow). C) Graphic depicting two point forces applied tangent to the surface of a sphere in the ± *x*-direction representing the angle adjust and drive gas flows (red and blue arrows respectively) and the resultant torque vector (black arrow). D) Computer-aided design (CAD) model of the entire pneumatic angle adjust stator, with the drive aperture highlighted in blue and the angle adjust aperture highlighted in red.

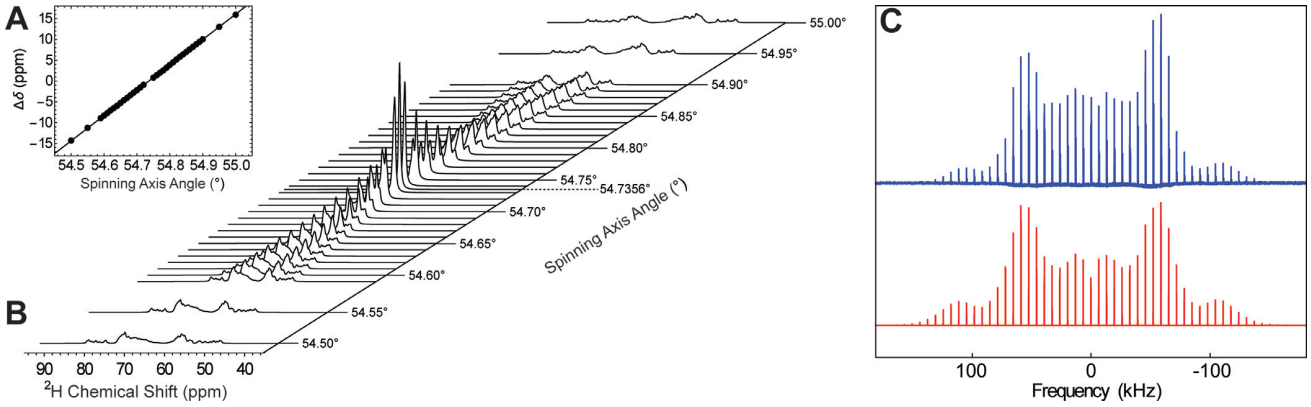

Fig. 2. A) Calibration curve of the spinning axis angle against the difference in ppm between the two inner peaks of the simulated off-angle sideband lineshape for the COOD ^{2}H resonance of d_4-malonic acid at 3000 Hz rotation rate. At values near the magic angle, the peaks are too close to one another to accurately measure a splitting. B) Simulated spectra for the 1st order sideband of the COOD ^{2}H resonance as a function of sample rotation angle at a rate of 3000 Hz, using a C_q value of 180 kHz and an η_q value of 0.11. C.) Experimental ^{2}H MAS spectrum of d_4-malonic acid (blue) at 6536 Hz MAS (2 bar helium gas) at the magic angle compared to a calculated ^{2}H MAS spectrum at the same MAS rate for a single ^{2}H resonance with C_q = 180 kHz and η_q = 0.11 (red).

pletely unstable when the gas flow rates from each aperture were similar in magnitude, likely due to turbulent interactions between the two gas streams within the stator cup. However, by placing the second aperture on the opposite side of the rotor (as adopted in the final design, shown in Fig. 1A), the two gas streams will not interfere with one another. If the second aperture were placed exactly 180^0 opposite the main drive aperture, an increase in the gas flow rate through that aperture would cause the spinning rate to increase, but with no change in spinning axis angle. Therefore, the angle adjust aperture must be slightly offset opposite the main drive aperture rotor in order to pitch the axis of rotation. As seen in Fig. 1A, at this chosen position, the angle adjust gas stream does not flow over the rotor grooves, but we have previously demonstrated that engagement with the grooves is not required in order to apply sufficient torque to the rotor [17].

Fig. 2B depicts simulated ^{2}H NMR spectra for the 1st order sideband of d_4-malonic acid as a function of spinning axis angle at 3000 Hz rotation rate. The quadrupole coupling constant, C_q, and asymmetry parameter, η_q, used for the simulations were set to 180 kHz and 0.11, respectively. These values were chosen to be close to the experimentally measured quadrupole parameters for the two nearly-identical COOD crystallographic sites within crystalline malonic acid, which have been previously determined to be C_q = 179.1 kHz, η_q = 0.112 for site 1 and C_q = 180.9 kHz, η_q = 0.098 for site 2 [37–39]. As a verification that the chosen quadrupolar parameters are suitable for the simulation, the full pattern under MAS was simulated using these values and compared to experiment by spinning the rotor at 6536 Hz using helium gas as shown in Fig. 2C. The sideband lineshape is highly dependent on the angle of the spinning axis with respect to the magnetic field, developing into a pattern with two peaks at angle values offset from the magic angle. The relative peak heights between the upfield and downfield resonances of the lineshape changes based on whether the angle is pitched above or below the magic angle. The center band also manifests as a splitting,

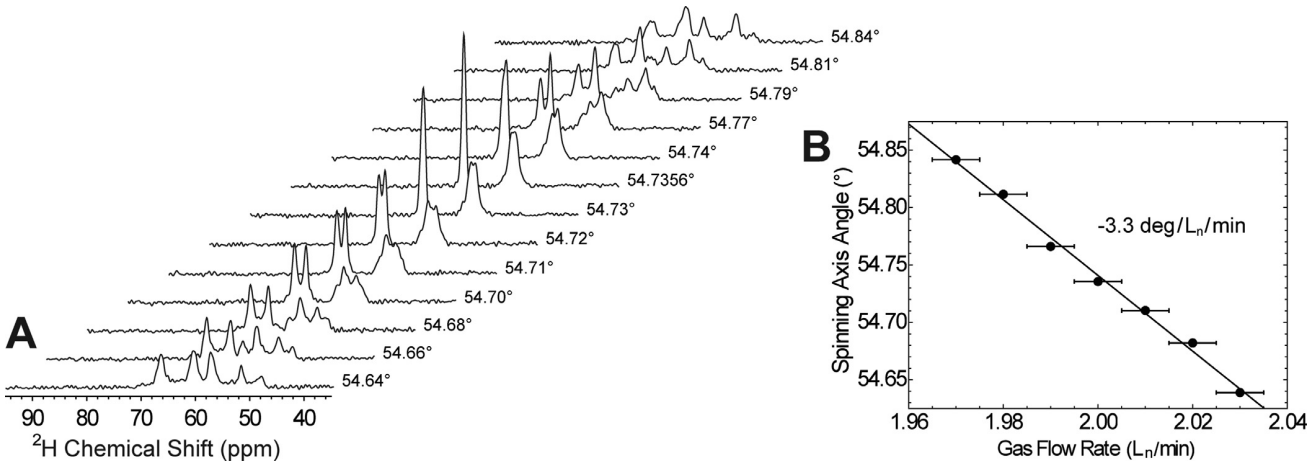

Fig. 3. A) ^{2}H NMR spectra of the first order sideband in d_4-malonic acid as a function of spinning angle at spinning rates ranging between 2869 Hz (54.64^0) and 2861 Hz (54.84^0), taken with 256 scans per spectrum. The first order sideband of the COOD resonance is centered at 63.4 ppm, and the first order sideband of the CD_2 resonance is centered at 54.3 ppm. The spinning angle for each spectrum was assigned based on the linear fit given in Eq. (1). B) Relationship between measured flow rate of air through the angle adjust aperture in liters normal per min (L_n/min) and the observed spinning angle for the spherical rotor.

but does not have a difference in peak heights between the upfield and downfield peaks as a function of absolute angle offset. A plot of the difference in chemical shift between the shorter and taller peak maxima as a function of spinning axis angle (in degrees) is shown in Fig. 2a, and a linear fit yields the following equation:

$$\Delta\delta = (60.835\ \text{ppm}/^\circ)\theta - 3329.88\ \text{ppm} \quad (1)$$

This linear fit is valid only for spinning rates near 3000 Hz where these spectra were simulated, as the off-magic angle lineshape for this resonance changes significantly as a function of spinning rate (Supplementary Information, Figs. S2, S3). For example, when spinning at 30 kHz, the first order sideband maintains the property of having an asymmetric lineshape dependent on absolute angle offset, but it no longer manifests as a peak splitting. At 100 kHz, the first order sideband no longer contains much information about angle offset other than through a narrowing of the linewidth at values near the magic angle. Though not sensitive to absolute offset, at high spinning rates the center band lineshape does manifest as a peak splitting when spinning off-magic angle. This makes the use of d_4-malonic acid or another deuterated organic solid an ideal and sensitive method for setting the magic angle even at extremely high MAS rates where other methods would fail (such as the measurement of rotor echoes in the ^{79}Br NMR signal of KBr), as it does not require observation of spinning sidebands. Currently, there is a dearth of reliable methods for setting the magic angle at high MAS rates, with the most effective method to date involving optimization of the intensity of ^{1}H signal obtained through a J-coupling mediated spin echo experiment [40]. It is worth noting that the malonic acid ^{2}H centerband and sideband lineshapes are not dependent on magnetic field strength, with simulated spectra effectively unchanging between 7 T and 21 T (Supplementary Information, Fig. S4).

The successful implementation of the pneumatic angle adjustment stator is shown by the results depicted in Fig. 3. The angle adjust gas flow rate was finely adjusted at values between 1.97 and 2.03 L normal of air per minute (L_n/min), yielding spectra which differ in spinning angle by 0.01^0 or less. The COOD resonance is the resonance at higher chemical shift (CD_2 is the resonance at lower chemical shift), and the angle for each spectrum was assigned based on the peak splitting for this COOD resonance using Eq. (1). The sensitivity of the angle adjustment capability of the stator was measured by taking the linear fit of the measured flow rate values as they correspond to rotor spinning axis angles, resulting in a sensitivity of -3.3 ± 0.1^0 per L_n/min of flow. The needle valve used in the experimental setup was capable of restricting the flow at increments finer than the measurement precision of the digital flow meter used (± 5 mL_n/min), meaning that the major contribution of error to the linear fit in Fig. 3B was from the flow rate measurement. As predicted, a small but measurable linear change in spinning rate coincided with the change in gas flow rate, with a spinning rate of 2861 Hz at 54.84^0 with 1.97 L_n/min of air, and a rate of 2869 Hz at 54.64^0 and 2.03 L_n/min of air. The spinning rate was extremely stable, varying by less than ± 1 Hz at each angle adjustment gas flow rate value. As a result of the linear relationship between spinning rate and spinning angle, use of feedback-based control (PID control) of the spinning rate based on the optical tachometer signal also controls the angle of the rotational axis to a desired value. By changing properties of the angle adjustment aperture such as its placement within the stator cup, its size, or the radial distance from the aperture to the rotor's surface, the angle adjustment sensitivity could be modified to suit the desired technical requirements for a given experiment.

Conclusion

We have demonstrated for the first time a pneumatic angle adjustment method of rotors for MAS solid state NMR experiments that involves no moving parts other than the rotor itself. This technique is made possible by the use of spherical rotors and represents a unique and novel advantage that spherical rotors have over cylindrical rotors. We have also affirmed the utility of using a deuterated organic solid such as d_4-malonic acid as a very precise and absolute angle measurement standard sample for solid state NMR experiments. The capability for spherical rotors to pitch within the stator with no mechanical adjustment may enable the design of new probeheads that utilize a monolithic RF circuit with precisely defined geometries, or may simply free up space to make smaller and more technically complex probeheads. Future work will entail further developing the pneumatic angle adjustment stator to be capable of performing variable angle spinning (VAS) experiments from 0^0 to 90^0 [41], or dynamic-angle spinning (DAS, also known as switched-angle spinning or SAS) experiments [32,34,42–45], which could be made possible by rapidly gating the gas flow through the angle adjustment aperture.

Declaration of Competing Interest

ETH Zürich has filed intellectual property protection of the invention described herein. A.B.B. is an author on provisional patents related to this work filed by Washington University in Saint Louis (62/703,278

filed on 25 July 2018 and 62/672,840 filed on 17 May 2018). The authors declare no other competing interests.

Acknowledgments

This research was supported by start-up funding from ETH Zürich. We thank Dr. John Griffin (Lancaster University) for valuable discussions and advice regarding the use of d_4-malonic acid as an observable for spinning angle adjustment.

Supplementary materials

Supplementary material associated with this article can be found, in the online version, at doi:10.1016/j.jmro.2021.100014.

References

[1] E.R. Andrew, A. Bradbury, R.G. Eades, Removal of dipolar broadening of nuclear magnetic resonance spectra of solids by specimen rotation, Nature 183 (1959) 1802–1803, doi:10.1038/1831802a0.
[2] I.J. Lowe, Free induction decays of rotating solids, Phys. Rev. Lett. 2 (1959) 285–287, doi:10.1103/PhysRevLett.2.285.
[3] E.R. Andrew, Magic angle spinning, Int. Rev. Phys. Chem. 1 (1981) 195–224, doi:10.1080/01442358109353320.
[4] M.M. Maricq, J.S. Waugh, NMR in rotating solids, J. Chem. Phys. 70 (1979) 3300–3316, doi:10.1063/1.437915.
[5] D.D. Laws, H.-M.L. Bitter, A. Jerschow, Solid-state NMR spectroscopic methods in chemistry, Angew. Chem. Int. Ed. 41 (2002) 3096–3129, doi:10.1002/1521-3773(20020902)41:17>3096::AID-ANIE3096<3.0.CO;2-X.
[6] S.E. Ashbrook, M.J. Duer, Structural information from quadrupolar nuclei in solid state NMR, Concepts Magn. Reson. Part A. 28A (2006) 183–248, doi:10.1002/cmr.a.20053.
[7] A.P.M. Kentgens, A practical guide to solid-state NMR of half-integer quadrupolar nuclei with some applications to disordered systems, Geoderma 80 (1997) 271–306, doi:10.1016/S0016-7061(97)00056-6.
[8] K.A. Collier, S. Sengupta, C.A. Espinosa, J.E. Kelly, J.I. Kelz, R.W. Martin, Design and construction of a quadruple-resonance MAS NMR probe for investigation of extensively deuterated biomolecules, J. Magn. Reson. 285 (2017) 8–17, doi:10.1016/j.jmr.2017.10.002.
[9] N. Alaniva, E.P. Saliba, E.L. Sesti, P.T. Judge, A.B. Barnes, Electron decoupling with chirped microwave pulses for rapid signal acquisition and electron saturation recovery, Angew. Chem. – Int. Ed. 58 (2019) 7259–7262, doi:10.1002/anie.201900139.
[10] F.J. Scott, E.P. Saliba, B.J. Albert, N. Alaniva, E.L. Sesti, C. Gao, N.C. Golota, E.J. Choi, A.P. Jagtap, J.J. Wittmann, M. Eckardt, W. Harneit, B. Corzilius, S. Th. Sigurdsson, A.B. Barnes, Frequency-agile gyrotron for electron decoupling and pulsed dynamic nuclear polarization, J. Magn. Reson. 289 (2018) 45–54, doi:10.1016/j.jmr.2018.02.010.
[11] E.L. Sesti, N. Alaniva, P.W. Rand, E.J. Choi, B.J. Albert, E.P. Saliba, F.J. Scott, A.B. Barnes, Magic angle spinning NMR below 6 K with a computational fluid dynamics analysis of fluid flow and temperature gradients, J. Magn. Reson. 286 (2018) 1–9, doi:10.1016/j.jmr.2017.11.002.
[12] R.W. Martin, E.K. Paulson, K.W. Zilm, Design of a triple resonance magic angle sample spinning probe for high field solid state nuclear magnetic resonance, Rev. Sci. Instrum. 74 (2003) 3045–3061, doi:10.1063/1.1571951.
[13] F.D. Doty, Solid state NMR probe design, Encycl. Magn. Reson. (2007) 1–21, doi:10.1002/9780470034590.emrstm1001.
[14] T. Matsunaga, T. Mizuno, K. Takegoshi, An X0 shim coil for precise magic-angle adjustment, J. Magn. Reson. 256 (2015) 1–8, doi:10.1016/j.jmr.2015.04.007.
[15] P. Chen, B.J. Albert, C. Gao, N. Alaniva, L.E. Price, F.J. Scott, E.P. Saliba, E.L. Sesti, P.T. Judge, E.W. Fisher, A.B. Barnes, Magic angle spinning spheres, Sci. Adv. 4 (2018) 1–8, doi:10.1126/sciadv.aau1540.
[16] C. Gao, P.T. Judge, E.L. Sesti, L.E. Price, N. Alaniva, E.P. Saliba, B.J. Albert, N.J. Soper, P.H. Chen, A.B. Barnes, Four millimeter spherical rotors spinning at 28 kHz with double-saddle coils for cross polarization NMR, J. Magn. Reson. 303 (2019) 1–6, doi:10.1016/j.jmr.2019.03.006.
[17] T.M. Osborn Popp, A. Däpp, C. Gao, P. Chen, L.E. Price, N.H. Alaniva, A.B. Barnes, Highly stable magic angle spinning spherical rotors, Magn. Reson. 1 (2020) 97–103, doi:10.5194/mr-1-97-2020.
[18] Z. Gan, Isotropic NMR spectra of half-integer quadrupolar nuclei using satellite transitions and magic-angle spinning, J. Am. Chem. Soc. 122 (2000) 3242–3243, doi:10.1021/ja9939791.
[19] Z. Gan, Satellite transition magic-angle spinning nuclear magnetic resonance spectroscopy of half-integer quadrupolar nuclei, J. Chem. Phys. 114 (2001) 10845–10853, doi:10.1063/1.1374958.
[20] S.E. Ashbrook, S. Wimperis, High-resolution NMR spectroscopy of quadrupolar nuclei in solids: satellite-transition MAS with self-compensation for magic-angle misset, J. Am. Chem. Soc. 124 (2002) 11602–11603, doi:10.1021/ja0203869.
[21] C. Huguenard, F. Taulelle, B. Knott, Z. Gan, Optimizing STMAS, J. Magn. Reson. 156 (2002) 131–137, doi:10.1006/jmre.2002.2548.
[22] G. Pileio, Y. Guo, T.N. Pham, J.M. Griffin, M.H. Levitt, S.P. Brown, Residual dipolar couplings by off-magic-angle spinning in solid-state nuclear magnetic resonance spectroscopy, J. Am. Chem. Soc. 129 (2007) 10972–10973, doi:10.1021/ja0721115.
[23] J. Courtieu, J.P. Bayle, B.M. Fung, Variable angle sample spinning NMR in liquid crystals, Prog. Nucl. Magn. Reson. Spectrosc. 26 (1994) 141–169, doi:10.1016/0079-6565(94)80006-5.
[24] O. Weintraub, S. Vega, Dynamic 2H nuclear magnetic resonance of rotating solids, Solid State Nucl. Magn. Reson. 4 (1995) 341–351, doi:10.1016/0926-2040(95)00007-D.
[25] Y. Huang, R.L. Vold, G.L. Hoatson, Investigation of multiaxis molecular motion by off-magic angle spinning deuteron NMR, J. Chem. Phys. 124 (2006) 104504, doi:10.1063/1.2162544.
[26] M. Blackledge, Recent progress in the study of biomolecular structure and dynamics in solution from residual dipolar couplings, Prog. Nucl. Magn. Reson. Spectrosc. 46 (2005) 23–61, doi:10.1016/j.pnmrs.2004.11.002.
[27] G. Bodenhausen, P. Caravatti, J. Deli, R.R. Ernst, H. Sauter, Optical alignment in magic-angle NMR, J. Magn. Reson. 48 (1982) 143–147, doi:10.1016/0022-2364(82)90246-3.
[28] E. Mihaliuk, T. Gullion, Optical lever for monitoring of the magic angle, J. Magn. Reson. 223 (2012) 46–50, doi:10.1016/j.jmr.2012.08.007.
[29] S. Mamone, A. Dorsch, O.G. Johannessen, M.V Naik, P.K. Madhu, M.H. Levitt, A Hall effect angle detector for solid-state NMR, J. Magn. Reson. 190 (2008) 135–141, doi:10.1016/j.jmr.2007.07.012.
[30] J.S. Frye, G.E. Maciel, Setting the magic angle using a quadrupolar nuclide, J. Magn. Reson. 48 (1982) 125–131, doi:10.1016/0022-2364(82)90243-8.
[31] G.L. Hoatson, R.L. Vold, 2H-NMR spectroscopy of solids and liquid crystals, in: Solid-State NMR III Organic Matter, Springer, Berlin, Heidelberg, 1994, pp. 1–67, doi:10.1007/978-3-642-61223-7_1.
[32] K.T. Mueller, G.C. Chingas, A. Pines, NMR probe for dynamic-angle spinning, Rev. Sci. Instrum. 62 (1991) 1445–1452, doi:10.1063/1.1142465.
[33] J.M. Griffin, J.R. Yates, A.J. Berry, S. Wimperis, S.E. Ashbrook, High-resolution 19F MAS NMR spectroscopy: structural disorder and unusual J couplings in a fluorinated hydroxy-silicate, J. Am. Chem. Soc. 132 (2010) 15651–15660, doi:10.1021/ja105347q.
[34] I.M. Litvak, C.A. Espinosa, R.A. Shapiro, A.N. Oldham, V.V. Duong, R.W. Martin, Pneumatic switched angle spinning NMR probe with capacitively coupled double saddle coil, J. Magn. Reson. 206 (2010) 183–189, doi:10.1016/j.jmr.2010.07.001.
[35] M. Bak, J.T. Rasmussen, N.C. Nielsen, SIMPSON: a general simulation program for solid-state NMR spectroscopy, J. Magn. Reson. 147 (2000) 296–330, doi:10.1006/jmre.2000.2179.
[36] D. Massiot, F. Fayon, M. Capron, I. King, S.Le Calvé, B. Alonso, J. Durand, B. Bujoli, Z. Gan, G. Hoatson, Modelling one- and two-dimensional solid-state NMR spectra, Magn. Reson. Chem. 40 (2002) 70–76, doi:10.1002/mrc.984.
[37] W. Derbyshire, T.C. Gorvin, D. Warner, A deuteron magnetic resonance study of a single crystal of deuterated malonic acid, Mol. Phys. 17 (1969) 401–407, doi:10.1080/00268976900101191.
[38] C. Müller, S. Idziak, N. Piślewski, U. Haeberlen, Deuteron NMR on single crystals. EFGs, signs of quadrupole coupling constants, and assignment of σ tensors in malonic acid, J. Magn. Reson. 47 (1982) 227–239, doi:10.1016/0022-2364(82)90116-0.
[39] S. Idziak, N. Piślewski, An NMR relaxation study on the hydrogen dynamics in malonic acid, Chem. Phys. 111 (1987) 439–443, doi:10.1016/0301-0104(87)85091-7.
[40] S. Penzel, A.A. Smith, M. Ernst, B.H. Meier, Setting the magic angle for fast magic-angle spinning probes, J. Magn. Reson. 293 (2018) 115–122, doi:10.1016/j.jmr.2018.06.002.
[41] L. Frydman, G.C. Chingas, Y.K. Lee, P.J. Grandinetti, M.A. Eastman, G.A. Barrall, A. Pines, Correlation of isotropic and anisotropic chemical shifts in solids by two-dimensional variable-angle-spinning NMR, Isr. J. Chem. 32 (1992) 161–164, doi:10.1002/ijch.199200022.
[42] A. Bax, N.M. Szeverenyi, G.E. Maciel, Chemical shift anisotropy in powdered solids studied by 2D FT NMR with flipping of the spinning axis, J. Magn. Reson. 55 (1983) 494–497, doi:10.1016/0022-2364(83)90134-8.
[43] T. Terao, T. Fujii, T. Onodera, A. Saika, Switching-angle sample-spinning NMR spectroscopy for obtaining powder-pattern-resolved 2D spectra: Measurements of 13C chemical-shift anisotropies in powdered 3,4-dimethoxybenzaldehyde, Chem. Phys. Lett. 107 (1984) 145–148, doi:10.1016/0009-2614(84)85689-4.
[44] M.. Eastman, P.. Grandinetti, Y.. Lee, A. Pines, Double-tuned hopping-coil probe for dynamic-angle-spinning NMR, J. Magn. Reson. 98 (1992) 333–341, doi:10.1016/0022-2364(92)90136-U.
[45] G. Zandomeneghi, M. Tomaselli, J.D. Van Beek, B.H. Meier, Manipulation of the director in bicellar mesophases by sample spinning: a new tool for NMR spectroscopy, J. Am. Chem. Soc. 123 (2001) 910–913, doi:10.1021/ja0019326.